

2011

Modeling of solvent evaporation from polymer jets in electrospinning

Xiang-Fa Wu

University of Nebraska-Lincoln

Yury Salkovskiy

University of Nebraska-Lincoln

Yuris A. Dzenis

University of Nebraska-Lincoln, ydzenis@unl.edu

Follow this and additional works at: <http://digitalcommons.unl.edu/mechengfacpub>



Part of the [Mechanics of Materials Commons](#), [Nanoscience and Nanotechnology Commons](#), [Other Engineering Science and Materials Commons](#), and the [Other Mechanical Engineering Commons](#)

Wu, Xiang-Fa; Salkovskiy, Yury; and Dzenis, Yuris A., "Modeling of solvent evaporation from polymer jets in electrospinning" (2011). *Mechanical & Materials Engineering Faculty Publications*. 106.
<http://digitalcommons.unl.edu/mechengfacpub/106>

This Article is brought to you for free and open access by the Mechanical & Materials Engineering, Department of at DigitalCommons@University of Nebraska - Lincoln. It has been accepted for inclusion in Mechanical & Materials Engineering Faculty Publications by an authorized administrator of DigitalCommons@University of Nebraska - Lincoln.

Modeling of solvent evaporation from polymer jets in electrospinning

Xiang-Fa Wu,^{a)} Yury Salkovskiy,^{b)} and Yuris A. Dzenis^{c)}

Department of Engineering Mechanics and Nebraska Center for Materials and Nanoscience, Nanofiber Facility, University of Nebraska–Lincoln, Lincoln, Nebraska 68588-0526, USA

(Received 24 March 2011; accepted 12 April 2011; published online 2 June 2011)

Solvent evaporation plays a critical role in nanofiber formation in electrospinning. Here, we present a nonlinear mass diffusion-transfer model describing the drying process in dilute polymer solution jets. The model is used to predict transient solvent concentration profiles in polyacrylonitrile/*N,N*-dimethylformamide (PAN/DMF) jets with the initial radii ranging from 50 μm down to 100 nm. Numerical simulations demonstrate high transient inhomogeneity of solvent concentration over the jet cross-section in microscopic jets. The degree of inhomogeneity decreases for finer, submicron jets. The simulated jet drying time decreases rapidly with the decreasing initial jet radius, from seconds for microjets to single milliseconds for nanojets. The results demonstrate the need for further improved coupled multiphysics models of electrospinning jets. © 2011 American Institute of Physics. [doi:10.1063/1.3585148]

Electrospinning is an established nanomanufacturing technology producing continuous nanofibers from polymer solutions in high electric fields.^{1–3} Worldwide interest in the electrospinning process and continuous nanofibers is growing rapidly and nanofiber applications in advanced composites, filters, catalytic membranes, protective clothing, biomedical scaffolds, rechargeable batteries, and other areas^{4–7} are being explored and developed.

Electrospinning is a complex, multiphysics process involving electrohydrodynamics, mass and heat diffusion and transfer, and solidification. This process can be subdivided into several stages, i.e., jet initiation,^{8,9} steady-state jet motion,^{10–13} jet instabilities,^{14–16} and nanofiber deposition. Several studies have been conducted to understand the first three stages and a number of electrohydrodynamic models have been developed.^{8–16} Yet, these models were all built on the assumption of a homogeneous jet. In electrospinning, solvent evaporation from jet surface may lead to jet inhomogeneity in the radial direction in dilute polymer jets. Solvent evaporation can be fast in ultrafine jets typical for electrospinning. Rapid solvent evaporation accompanied by jet stretching due to electric forces and jet instabilities is ultimately responsible for the diameter, structure, and properties of the final solidified nanofibers. Solvent evaporation is also most likely the cause of the observed fiber skins, flat ribbons, and porous nanofibers in electrospinning.^{17,18}

Solvent evaporation from polymer coatings and films has been extensively studied based on Fick's law of mass diffusion.^{19–23} For polymer jets in dry fiber spinning, a few studies have been conducted on the steady-state temperature and solvent concentrations in the jets.^{24–27} Recent electrospinning experiments with controlled environmental humidity have demonstrated the importance of solvent evaporation to nanofiber formation.²⁸ Nevertheless, kinetics of solvent evaporation from electrospun jets has not yet been studied.

Unlike flat films, evaporation-induced surface contraction in dilute electrospun jets can result in significant surface area decrease that will affect the mass transfer rate at the free surface.

The following assumptions are used to derive the governing equations for solvent evaporation from thin polymer jets:^{19,20} (1) no temperature gradient exists inside the jet; (2) the mass diffusion and transfer is axisymmetric; (3) microconvection due to concentration gradients is negligible; and (4) no chemical reactions take place inside the jet.

For a binary polymer solution, the total volume-average diffusion velocity u_V is $u_V = C_1 \bar{V}_1 u_1 + C_2 \bar{V}_2 u_2$, where C_1 and C_2 , \bar{V}_1 and \bar{V}_2 , and u_1 and u_2 are the mass concentrations, specific partial volumes, and diffusive velocities of the two components of the mixture, respectively. Herein, variables with subscript 1 are chosen to denote those related to solvent, while variables with subscript 2 indicate those related to polymer. The mass concentration C_i ($i=1,2$) and the specific partial volume V_i ($i=1,2$) of the solution constituents are

$$C_i = M_i/V, V_i = \partial V / \partial M_i|_{T,P,M} \quad (i=1,2), \quad (1)$$

where V is the total volume of the mixture. The partial specific volumes of the two constituents are assumed to be independent of their compositions, thus no volume change happens during the mixing process. The partial specific volume \bar{V} (cm^3/g) is the reciprocal of mass density ρ : $\bar{V}_i = 1/\rho_i$ ($i=1,2$). The diffusive flux of each constituent with respect to the total volume-average velocity is $j_i = C_i(u_i - u_V)$ ($i=1,2$). Mass (volume) conservation of the mixture requires $C_1 \bar{V}_1 + C_2 \bar{V}_2 = 1$. The axisymmetric Fick's law of mass diffusion in the radial direction gives

$$j_i = -D \partial C_i / \partial r, \quad (2)$$

where D (cm^2/g) is the mass diffusivity. Continuity of the mixture leads to the governing equation of mass diffusion in the jet

$$\frac{\partial C_1}{\partial t} = \frac{1}{r} \frac{\partial}{\partial r} \left(D r \frac{\partial C_1}{\partial r} \right). \quad (3)$$

Initial conditions at the beginning of the drying process are

^{a)}Current address: Department of Mechanical Engineering, North Dakota State University, Fargo, ND 58108.

^{b)}Current address: Department of Mathematical Theory of Elasticity and Biomechanics, Saratov State University, Saratov, Russia.

^{c)}Author to whom correspondence should be addressed: Electronic mail: ydzenis@unl.edu.

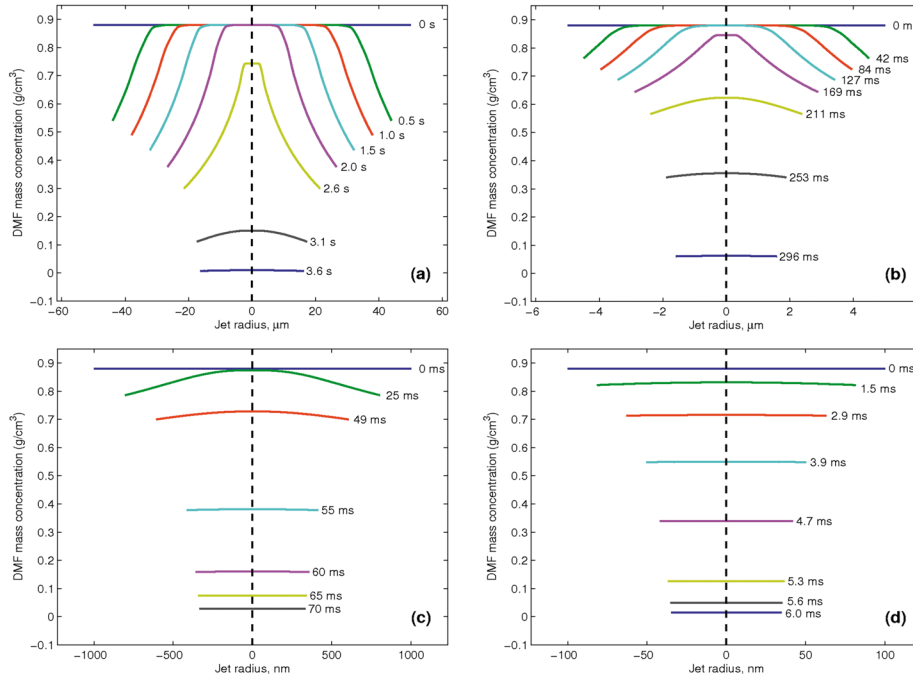


FIG. 1. (Color online) Evolution of solvent (DMF) mass concentration profile in jets with initial radius: $R_0 = 50 \mu\text{m}$ (a), $5 \mu\text{m}$ (b), $1 \mu\text{m}$ (c), and 100 nm (d).

$$t = 0: \quad C_1 = C_{10}, \quad R(0) = R_0. \quad (4)$$

Boundary conditions at the center and moving surface of the jet are

$$r = 0: \quad \partial C_1 / \partial r = 0, \quad (5)$$

$$r = R(t): \quad \frac{D}{1 - \bar{V}_1 C_1} \frac{\partial C_1}{\partial r} = - \frac{k_g M_1 (P_s - P_\infty)}{R_g T}, \quad (6)$$

$$r = R(t): \quad \frac{dR(t)}{dt} = - \frac{k_g M_1 \bar{V}_1}{R_g T} (P_s - P_\infty). \quad (7)$$

In the above, C_{10} is the initial solvent mass concentration which is treated as constant over the jet cross-section; R_0 is the initial jet radius; $R(t)$ is the current jet radius; k_g (cm/g) is the coefficient of solvent mass transfer at the jet surface; M_1 is the solvent molar weight; T is the absolute temperature near the surface; $R_g = 8.3144 \text{ J/mol}$ is the universal gas constant; P_∞ is the solvent vapor pressure in the atmosphere far from the jet surface ($P_\infty = 0$ in this study); and P_s is the solvent saturation vapor pressure near the jet surface. The dependence of P_s on the solvent concentration near the jet surface can be estimated according to the Flory–Huggins equation:²⁹ $P_s/P_0 = \phi_1 \exp(\phi_2 + \chi \phi_2^2)$, where P_0 is the saturation vapor pressure of the pure solvent, ϕ_1 and ϕ_2 ($\phi_2 = 1 - \phi_1$) are the solvent and polymer volume fractions, respectively, and χ is the Flory–Huggins polymer/solvent interaction parameter. χ can be approximated by using Bristow's semiempirical equation:³⁰ $\chi = 0.35 + (\delta_1 - \delta_2)^2 \bar{V} / (R_g T)$, where \bar{V} is the solvent molar volume, and δ_1 and δ_2 are the solubility parameters of the solvent and polymer, respectively. In this study, χ is selected as a constant, i.e., $\chi = 0.45$. The polymer/solvent mutual diffusivity D is described by the Vrentas–Duda free-volume theory:²³ $D = D_1 (1 - \phi_1)^2 (1 - 2\chi \phi_1)$, where D_1 is the solvent self-diffusion coefficient.

To formulate a robust, efficient numerical method, moving grids are introduced to describe the large jet contraction.

A polar r -coordinate axis is attached on the polymer at each time step in the numerical iteration, by analogy with Ref. 31. The change rate of solvent mass concentration at grid r_i is

$$\left(\frac{\partial C_1}{\partial t} \right)_i = \left(\frac{\partial C_1}{\partial r} \right)_i \left(\frac{dr}{dt} \right)_i + \left(\frac{\partial C_1}{\partial t} \right)_r, \quad (8)$$

where C_1 is a function with respect to time t and grid coordinate r_i . With the aid of Fick's law and the simple mixture rule, the polymer radial velocity at grid r_i is

$$\left(\frac{dr}{dt} \right)_i = \frac{D \bar{V}_1}{1 - \bar{V}_1 C_1} \left(\frac{\partial C_1}{\partial r} \right)_i. \quad (9)$$

Substitution of Eqs. (3) and (9) into Eq. (8) yields the mass diffusion equation

$$\left(\frac{\partial C_1}{\partial t} \right)_i = \frac{D \bar{V}_1}{1 - \bar{V}_1 C_1} \left(\frac{\partial C_1}{\partial r} \right)_i^2 + \frac{1}{r} \frac{\partial}{\partial r} \left(D r \frac{\partial C_1}{\partial r} \right)_r. \quad (10)$$

The above equation can be solved efficiently by means of the explicit backward-finite difference method.³²

To demonstrate the effectiveness of the model, we consider the drying process in PAN/DMF jets with the initial DMF mass concentration 88%. Evolution of the DMF concentration profile and jet radius as well as jet drying time as a function of the initial jet radius varying from $50 \mu\text{m}$ down to 100 nm are considered.

The parameters used in the simulations are as follows. The mass densities of DMF ($M_w = 73$) and PAN ($M_w = 150,000$) are $\rho_{\text{DMF}} = 0.944 \text{ g/cm}^3$ and $\rho_{\text{PAN}} = 1.184 \text{ g/cm}^3$, respectively. The PAN diffusion coefficient in infinite DMF is $D_1 = \sim 1.5 \times 10^{-6} \text{ cm}$. The DMF saturation vapor pressure at $20 \text{ }^\circ\text{C}$ is $\sim 500 \text{ Pa}$.³³ The DMF mass transfer coefficient at the jet surface is $k_g = \sim 0.2 \text{ m/s}$, by analogy with similar solvents.³⁴ The initial DMF mass ratio of 88% corresponds to $C_1 = 0.851$.

Figure 1 shows the evolution of DMF concentration profile in microscopic and submicrometer jets. It can be observed that solvent evaporation induces high transient con-

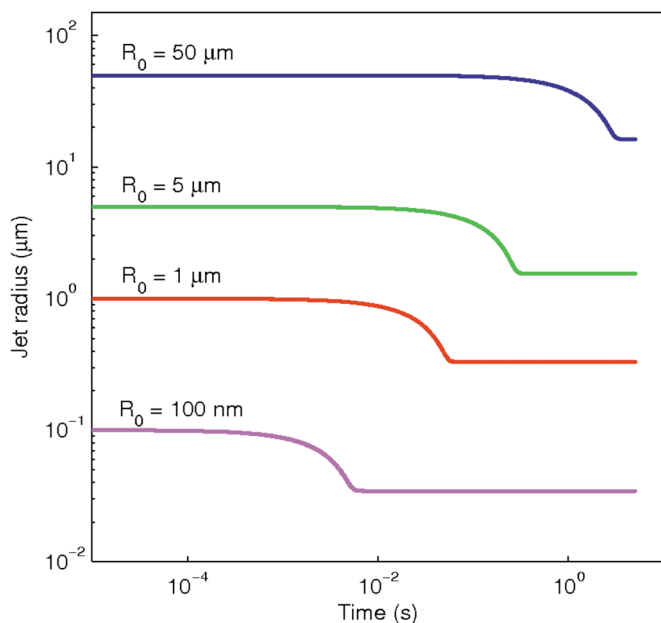


FIG. 2. (Color online) Time evolution of polymer jet radius as a result of solvent evaporation for initial jet radii: $R_0=50, 5,$ and $1 \mu\text{m}$ and 100 nm .

centration inhomogeneity in microscopic jets; the degree of inhomogeneity decreases with the initial jet radius decrease. Mass diffusion and transfer coefficients are the main controlling parameters.

Figure 2 plots the time history of PAN/DMF jet radii for microscopic and submicrometer jets. Interestingly, all the jet radii decrease in a similar fashion. Figure 3 shows the variation in the drying time with the initial jet radius. The drying time was defined as the time needed to evaporate 98% of the solvent. The simulations show rapid decrease in drying time from seconds for microscopic jets down to single milliseconds for jets with submicron initial radius.

The developed nonlinear mass diffusion-transfer model can be used to predict the drying times and compositional inhomogeneity in dilute polymer solution jets in electrospinning; such information is crucial to better process control and nanofiber optimization. The highly inhomogeneous concen-

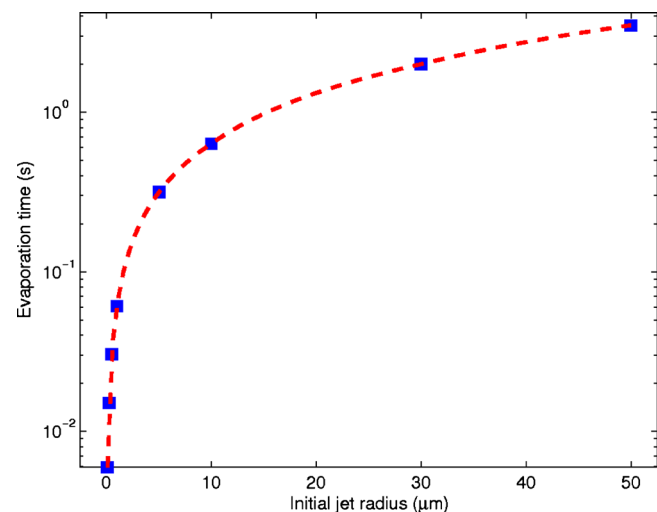


FIG. 3. (Color online) Variation in the jet drying time with the initial jet radius.

tration profiles will have a profound influence on the rheological and flow behavior of jets and need to be taken into account in the analysis of electrohydrodynamics of jet motion in electrospinning. The presented results, therefore, demonstrate the need for further development of improved multiphysics models of electrospun jets incorporating solvent evaporation.

This work was supported in part by grants from the National Science Foundation, DARPA/DSO (through a subcontract from Hexcel Corp No. HR0011-06-C-0011), and Nebraska Research Initiative Nanofiber Core Facility grant. The views expressed are those of the authors and do not reflect the official policy or position of the Department of Defense or the U. S. Government. This paper has been approved for public release.

¹Y. Dzenis, *Science* **304**, 1917 (2004).

²D. H. Reneker and I. Chun, *Nanotechnology* **7**, 216 (1996).

³J. Doshi and D. H. Reneker, *J. Electrostat.* **35**, 151 (1995).

⁴J. S. Kim and D. H. Reneker, *Polym. Compos.* **20**, 124 (1999).

⁵Y. Dzenis, *Science* **319**, 419 (2008).

⁶Y. Dzenis and Y. Wen, *Mater. Res. Soc. Symp. Proc.* **702**, U5.4.1 (2002).

⁷Z. M. Huang, Y. Z. Zhang, M. Kotaki, and S. Ramakrishna, *Compos. Sci. Technol.* **63**, 2223 (2003).

⁸A. F. Spivak and Y. A. Dzenis, *J. Appl. Mech.* **66**, 1026 (1999).

⁹A. L. Yarin, S. Koombhongse, and D. H. Reneker, *J. Appl. Phys.* **90**, 4836 (2001).

¹⁰A. F. Spivak and Y. A. Dzenis, *Appl. Phys. Lett.* **73**, 3067 (1998).

¹¹A. F. Spivak, Y. A. Dzenis, and D. H. Reneker, *Mech. Res. Commun.* **27**, 37 (2000).

¹²J. J. Feng, *Phys. Fluids* **14**, 3912 (2002).

¹³J. J. Feng, *J. Non-Newtonian Fluid Mech.* **116**, 55 (2003).

¹⁴D. H. Reneker, A. L. Yarin, H. Fong, and S. Koombhongse, *J. Appl. Phys.* **87**, 4531 (2000).

¹⁵M. M. Hohman, M. Shin, G. Rutledge, and M. P. Brenner, *Phys. Fluids* **13**, 2201 (2001).

¹⁶M. M. Hohman, M. Shin, G. Rutledge, and M. P. Brenner, *Phys. Fluids* **13**, 2221 (2001).

¹⁷S. Koombhongse, W. Liu, and D. H. Reneker, *J. Polym. Sci., Part B: Polym. Phys.* **39**, 2598 (2001).

¹⁸M. Bognitzki, W. Czado, T. Frese, A. Schaper, M. Hellwig, M. Steinhart, A. Greiner, and J. H. Wendorff, *Adv. Mater. (Weinheim, Ger.)* **13**, 70 (2001).

¹⁹R. Saure, G. R. Wagner, and E. U. Schlunder, *Surf. Coat. Technol.* **99**, 253 (1998).

²⁰R. Saure, G. R. Wagner, and E. U. Schlunder, *Surf. Coat. Technol.* **99**, 257 (1998).

²¹S. Alsoy and J. L. Duda, *AIChE J.* **45**, 896 (1999).

²²A. Indrakanti, N. Ramesh, J. L. Duda, and S. K. Kumar, *J. Chem. Phys.* **121**, 546 (2004).

²³J. L. Duda, J. S. Vrentas, S. T. Ju, and H. T. Liu, *AIChE J.* **28**, 279 (1982).

²⁴Y. Sano, *Drying Technol.* **2**, 167 (1983).

²⁵Y. Sano, *Drying Technol.* **19**, 1335 (2001).

²⁶Z. Gou and A. J. Mchugh, *J. Appl. Polym. Sci.* **87**, 2136 (2003).

²⁷Z. Gou and A. J. Mchugh, *J. Non-Newtonian Fluid Mech.* **118**, 121 (2004).

²⁸S. Tripatanasuwan, Z. X. Zhong, and D. H. Reneker, *Polymer* **48**, 5742 (2007).

²⁹P. J. Flory, *Principles of Polymer Chemistry* (Cornell University Press, Ithaca, 1953).

³⁰G. M. Bristow and W. F. Watson, *Trans. Faraday Soc.* **54**, 1731 (1958).

³¹J. Crank, *The Mathematics of Diffusion* (Oxford University Press, Oxford, 1975).

³²S. J. Farlow, *Partial Differential Equations for Scientists and Engineers* (Dover, New York, 1993).

³³*Handbook of Chemistry and Physics*, 82nd ed., edited by J. H. Lide (CRC, New York, 2001).

³⁴F. P. Incropera and D. P. DeWitt, *Fundamentals of Heat and Mass Transfer*, 4th ed. (Wiley, New York, 1996).